

Conventional description of Unconventional Coulomb-Crystal phase transition in three-dimensional classical $O(N)$ spin-ice

Senke Xu¹

¹*Department of Physics, Harvard University, Cambridge, MA 02138*

(Dated: November 3, 2018)

We study the phase transition between the high temperature Coulomb phase and the low temperature staggered crystal phase in three dimensional classical $O(N)$ spin-ice model. Compared with the previously proposed CP(1) formalism on the Coulomb-crystal transition of the classical dimer model, our description based on constrained order parameter is more conventional, due to a fundamental difference between the $O(N)$ and the dimer model. A systematic $\epsilon = 4 - d$ and $1/N$ expansion are used to study the universality class of the phase transition, and a stable fixed point is found based on our calculations for large enough N .

PACS numbers:

The three dimensional classical dimer model (CDM), as the simplest model with an algebraic liquid phase (usually called the Coulomb phase), has attracted many analytical and numerical studies [1, 2, 3, 4]. The ensemble of 3d CDM is all the configurations of dimer coverings, which are subject to a local constraint on every site: every site is connected to precisely n dimers with $0 < n < 6$ (denoted as CDM- n), and most studies are focused on the case with $n = 1$. The partition function of the CDM is a summation of all the allowed dimer coverings, with a Boltzmann weight that favors certain types of dimer configurations. For instance, the most standard CDM-1 takes the following form:

$$\begin{aligned} Z &= \sum_{\text{dimer configuration}} \exp\left(-\frac{E}{T}\right), \\ E &= \sum_{\text{plaquettes}} -U(n_{xy} + n_{yz} + n_{zx}). \end{aligned} \quad (1)$$

n_{xy} , n_{yz} and n_{zx} are numbers defined on each unit plaquette in xy , yz and zx planes, they take value 1 when this plaquette contains two parallel dimers, and take value 0 otherwise. When $U > 0$, the ground state of this model favors to have as many parallel dimers as possible, therefore when $T < T_c$, the system develops columnar crystalline dimer patterns in Fig. 1a, while when $T > T_c$ the system is in the Coulomb phase with power law correlation between dimer densities, which according to the standard Ginzburg-Landau theory can only occur at critical points instead of stable phases. This phase diagram has been confirmed by a number of numerical simulations [1, 2, 3, 4].

The nature of the transition at T_c attracts most efforts. If $U > 0$, numerical studies confirm that this transition is continuous, and the data suggest that at this transition the discrete cubic symmetry is enlarged to an $O(3)$ rotation symmetry [4]. Analytically, to describe this locally constrained dimer system, we can introduce the ‘‘magnetic field’’ $B_\mu = n_{i,+ \mu} \eta_i$, where $\eta_i = (-1)^i$ is a staggered sign distribution on the cubic lattice. The

number $n_{i,\mu}$ is defined on each link (i, μ) (Fig. 1a), and $n_{i,\mu} = 1, 0$ represents the presence and absence of dimer. Notice that link $(i, -\mu)$ and $(i-\mu, +\mu)$ are identical. Now the local constraint of the dimer system can be rewritten as a Gauss law constraint $\vec{\nabla} \cdot \vec{B}_i = \eta_i$. The mapping between the dimer pattern and the magnetic field configuration is depicted in Fig. 1. The standard way to solve this Gauss law constraint is to introduce vector potential \vec{A} defined on the unit plaquettes of the cubic lattice, and $\vec{B} = \vec{\nabla} \times \vec{A}$ [5, 6]. The background staggered magnetic charge η_i can be ignored in the Coulomb phase after coarse-graining, though it plays crucial role in the crystal phase. Since vector \vec{A} is no longer subject to any constraint, it is usually assumed that at low energy the system can be described by a local field theory of \vec{A} , for instance the field theory of the Coulomb phase reads $F \sim \int d^3x (\vec{\nabla} \times \vec{A})^2 + \dots$, which is invariant under gauge transformation $\vec{A} \rightarrow \vec{A} + \vec{\nabla} f$.

Now the Coulomb-crystal phase transition can be described by the condensation of the matter fields which couple minimally to the vector potential field \vec{A} : $\cos(\vec{\nabla} \theta^m - \vec{A})$, and mathematically this matter field is introduced because of the discrete nature of \vec{A} . Due to the staggered background magnetic charge η_i , the matter fields move on a nonzero background magnetic field, the band structure of the matter fields have multiple minima in the Brillouin zone, and the transformation between these minima encodes the information of the lattice symmetry. For instance the transition of the CDM-1 model is described by the CP(1) model with an enlarged SU(2) global symmetry [2, 7]. This field theory is highly unconventional, in the sense that it is not formulated in terms of physical order parameters. It is expected that more general CDM- n models can also be described by similar Higgs transition, although the detailed lattice symmetry transformation for matter fields would depend on n .

In this paper we will study an $O(N)$ generalization of the CDM model. We define an $O(N)$ spin vector S^a with unit length $\sum_a (S^a)^2 = 1$ on each link (i, μ) of the cubic

lattice, with $a = 1 \cdots N$, and we assume that the largest term of the Hamiltonian imposes an ice-rule constraint [8] for $O(N)$ spins on six links shared by every site:

$$\sum_{\mu=\pm x,\pm y,\pm z} S_{i,\mu}^a = 0. \quad (2)$$

Systems with this constraint is usually called the spin-ice. If $N = 1$, each spin can only take value ± 1 , therefore every site of the cubic lattice connects to three spins with $+1$ and three spins with -1 , which is equivalent to the CDM-3 model. Just like the CDM, at high temperature, there is a Coulomb phase with algebraic correlation between the $O(N)$ vector S^a , while the low temperature crystal phase is controlled by other interactions.

In addition to the large constraint Eq. 2, we can design the Hamiltonian as following:

$$E = \sum_{i,\mu,a} J_1 S_{i,-\mu}^a S_{i,\mu}^a + \sum_{i,a} \sum_{\mu \neq \nu} J_2 S_{i,\mu}^a S_{i+\nu,\mu}^a. \quad (3)$$

J_1 is a Heisenberg coupling between spins along the same lattice axis, J_2 is a Heisenberg coupling between spins on two parallel links across a unit square. If $J_1 > 0$ and $J_2 < 0$, in the ground state spins are antiparallel along the same axis, but parallel between parallel links across a unit square, which is an $O(N)$ analogue of the columnar state of the CDM in Fig. 1a. If J_1 and J_2 are both positive, in the ground state the spins are antiparallel between nearest neighbor links on the same axis, as well as between parallel links across a unit square, which is an analogue of the staggered dimer configuration in Fig. 1c. Since in the $J_1 - J_2$ model Eq. 3 there is no coupling between different axes along different directions, for both cases the zero temperature ground state of model Eq. 3 has large degeneracy, because the spins on x , y and z axes are ordered independently, and the energy does not depend on the relative angle between $S_{i,x}^a$, $S_{i,y}^a$ and $S_{i,z}^a$ *i.e.* the ground state manifold has an enlarged $[O(N)]^3$ symmetry. Compared with the dimer system, the $O(N)$ spin vector is not discrete, therefore we cannot use the Higgs mechanism as we did for the dimer model, which encodes the information of the discreteness of the dimer variables. Instead, we are going to describe the transition with a Ginzburg-Landau (GL) theory with order parameters. The applicability of our GL theory to the original CDM- n will be discussed later.

In this paper we will focus on the staggered spin order. Following the magnetic field formalism of the CDM mentioned before, in order to describe this system compactly, we introduce three flavors of $O(N)$ vector field $\phi_\mu^a = S_{i,+\mu}^a \eta_i$ with $\mu = x, y, z$, and now the constraint Eq. 2 can be rewritten concisely as

$$\sum_{\mu} \nabla_{\mu} \phi_{\mu}^a = 0. \quad (4)$$

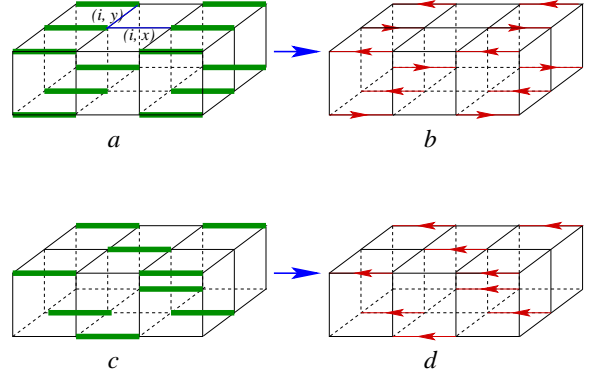


FIG. 1: (a), the low temperature columnar crystalline pattern of Eq. 1 studied in previous references; (b), the magnetic field distribution corresponding to this crystalline pattern (a), with a zero net magnetic field in the large scale; (c), the staggered dimer order; (d), the net nonzero magnetic field corresponding to the dimer crystal pattern in (c).

Under the lattice symmetry transformation, ϕ_μ^a transforms as

$$\begin{aligned} T_\mu &: \mu \rightarrow \mu + 1, \phi_\nu^a \rightarrow -\phi_\nu^a, \text{ (for all } \mu, \nu), \\ R_{\mu,s} &: \mu \rightarrow -\mu, \phi_\mu^a \rightarrow -\phi_\mu^a, \phi_\nu^a \rightarrow \phi_\nu^a, \text{ (for } \nu \neq \mu), \\ R_{\mu\nu} &: \mu \leftrightarrow \nu, \phi_\mu^a \leftrightarrow \phi_\nu^a, \text{ (for } \nu \neq \mu). \end{aligned} \quad (5)$$

T_μ is the translation symmetry along μ direction, $R_{\mu,s}$ is the site centered reflection symmetry, and $R_{\mu\nu}$ is the reflection along a diagonal direction.

The mapping between $S_{i,\mu}^a$ and ϕ_μ^a is very similar to the dimer case in Fig. 1, and the staggered spin order corresponds to the uniform order of ϕ_μ^a , and all flavors of spin vectors are ordered. Therefore presumably ϕ_μ^a are the low energy modes close to the transition, and we can write down the following symmetry allowed trial field theory for ϕ_μ^a with softened unit length constraint:

$$\mathcal{F} = \sum_{\mu,a} \phi_\mu^a (-\nabla^2 + r - \gamma \nabla_\mu^2) \phi_\mu^a + \sum_a g (\sum_{\mu} \nabla_{\mu} \phi_{\mu}^a)^2 + \mathcal{F}_4 \quad (6)$$

When we take $g \rightarrow \infty$, the constraint Eq. 4 is effectively imposed. In Eq. 6 when $\gamma = 0$, the quadratic part of the field theory is invariant under $O(N) \times O(3)$ transformation, the $O(3)$ symmetry is a combined flavor-space rotation symmetry. γ term will break the $O(3)$ symmetry down to the cubic lattice symmetry. However, to the accuracy of our calculation in this paper, the RG flow of γ is negligible. Therefore γ is a constant instead of a scaling function in the RG equation, we will tentatively take $\gamma = 0$ for simplicity. In the limit with $g \rightarrow \infty$, when $r > 0$ the correlation function of ϕ_μ^a reads:

$$\langle \phi_\mu^a(\vec{q}) \phi_\nu^b(-\vec{q}) \rangle \sim \frac{\delta_{ab}}{r + q^2} P_{\mu\nu}, \quad P_{\mu\nu} = \delta_{\mu\nu} - \frac{q_\mu q_\nu}{q^2}. \quad (7)$$

$P_{\mu\nu}$ is a projection matrix that projects a vector to the direction perpendicular to its momentum. After Fourier

transformation, this correlation function gives us the $1/r^3$ power-law spin correlation of the Coulomb phase. When $r < 0$, the vector ϕ_μ^a is ordered.

\mathcal{F}_4 in Eq. 6 includes all the symmetry allowed quartic terms of ϕ_μ^a :

$$\begin{aligned} \mathcal{F}_4 = & u \sum_{\mu} [\sum_a (\phi_\mu^a)^2]^2 + v \sum_{\mu \neq \nu} [\sum_a (\phi_\mu^a)^2] [\sum_b (\phi_\nu^b)^2] \\ & + w \sum_{\mu \neq \nu} [\sum_a \phi_\mu^a \phi_\nu^a] [\sum_b \phi_\mu^b \phi_\nu^b]. \end{aligned} \quad (8)$$

The u and v terms are invariant under an enlarged symmetry $[O(N)]^3$, while the w term breaks this symmetry down to one single $O(N)$ symmetry plus lattice symmetry. As already mentioned, the ground state manifold of model Eq. 3 has the same enlarged $[O(N)]^3$ symmetry. However, the w term can be induced with thermal fluctuation through order-by-disorder mechanism [9], or we can simply turn on such extra bi-quadratic term energetically in the $J_1 - J_2$ model Eq. 3. Just like the $J_1 - J_2$ model on the square lattice [9], the quadratic coupling $\sum_a \phi_\mu^a \phi_\nu^a$ with $\mu \neq \nu$ as well as more complicated quartic terms like $[\sum_a \phi_x^a \phi_y^a] [\sum_b \phi_y^b \phi_z^b]$ break the reflection symmetry of the system, and hence are forbidden.

Now a systematic renormalization group (RG) equation can be computed with four parameters u, v, w and r , at critical point $r = 0$ with the correlation function Eq. 7. In our calculation we will use $\epsilon = 4 - d$ expansion, and keep the accuracy to the first order ϵ expansion. Based on the spirit of ϵ expansion, all the loop integrals should be evaluated at $d = 4$, and because of the flavor-space coupling imposed by the constraint Eq. 2, we should generalize our system to four dimension, and also increase the flavor number to $\mu = 1 \cdots 4$. The full coupled RG equation reads

$$\begin{aligned} \frac{du}{d \ln l} &= \epsilon u - 5(8 + N)u^2 - \frac{17N}{4}v^2 - \frac{17}{4}w^2 \\ &\quad - (2 + N)uv - \frac{17}{2}vw - 3uw, \\ \frac{dv}{d \ln l} &= \epsilon v - \frac{2(4 + N)}{3}u^2 - \frac{52 + 37N}{6}v^2 - \frac{13}{6}w^2 \\ &\quad - \frac{34(2 + N)}{3}uv - 13vw - 14uw, \\ \frac{dw}{d \ln l} &= \epsilon w - \frac{8}{3}u^2 - \frac{2}{3}v^2 - \frac{33 + 7N}{3}w^2 \\ &\quad - 18vw - 20uw, \\ \frac{dr}{d \ln l} &= 2r - 6(2 + N)ur - 9Nvr - 9wr. \end{aligned} \quad (9)$$

Solving this equation at $r = 0$, we find stable fixed point for large enough N . Expanded to the order of ϵ/N^2 , the stable fixed point is located at

$$u_* = \frac{17\epsilon}{84N} - \frac{1139\epsilon}{441N^2} + O\left(\frac{\epsilon}{N^3}\right),$$

$$\begin{aligned} v_* &= -\frac{\epsilon}{42N} - \frac{1964\epsilon}{1323N^2} + O\left(\frac{\epsilon}{N^3}\right), \\ w_* &= \frac{3\epsilon}{7N} - \frac{4870\epsilon}{1323N^2} + O\left(\frac{\epsilon}{N^3}\right), \end{aligned} \quad (10)$$

This expansion is valid in the limit $\epsilon \sim 1/N^2 \ll 1$, and the fixed point values are determined by solving the equation Eq. 9 to the order of $\epsilon^2/N^2 \sim 1/N^6$. Close to the stable fixed point, the three eigenvectors of the RG flow have scaling dimensions

$$\begin{aligned} \Delta_1 &= -\epsilon + O\left(\frac{\epsilon}{N^2}\right), \\ \Delta_2 &= -\epsilon + \frac{4448\epsilon}{567N} + O\left(\frac{\epsilon}{N^2}\right), \\ \Delta_3 &= -\epsilon + \frac{24950\epsilon}{567N} + O\left(\frac{\epsilon}{N^2}\right). \end{aligned} \quad (11)$$

Δ_3 is the largest scaling dimension, and according to Eq. 11 the critical N is $N_c = 44$. In addition to this stable fixed point, there are seven other instable fixed points for $N > N_c$. For instance, in the large- N limit there is a fixed point at $u_* = \epsilon/(24N)$, $v_* = \epsilon/(12N)$ and $w_* = 0$, which has the enlarged $O(N) \times O(3)$ symmetry.

In the large- N limit, the RG equation for w is decoupled from u and v , hence four of the eight fixed points have $w_* = 0$, and all the others have $w_* = 3/(7N)$. If we take $w = w_* = 3/(7N)$, the RG flow diagram for u and v in the large- N limit is depicted in Fig. 2. At the stable fixed point Eq. 10, r is the only relevant perturbation, with scaling dimension

$$[r] = \frac{1}{\nu} = 2 - \epsilon + \frac{158\epsilon}{7N} + O\left(\frac{\epsilon}{N^2}, \epsilon^2\right) \quad (12)$$

Since at the ground state all three flavors of spin vectors are ordered, in the field theory \mathcal{F}_4 , v should be smaller than $2u$, which is well consistent with the stable fixed point in Eq. 10 with negative v_* . This fixed point has positive w_* , which favors noncollinear alignment between spins on different axes. Therefore the transition between Coulomb and noncollinear staggered state has a better chance to be described by this fixed point.

Notice that had we included the anisotropic velocity γ into account, its leading RG flow will be at order of $\epsilon^2/N \sim 1/N^5$, and the flow of γ will contribute to the RG flow of u, v and w at order of $\epsilon^3/N^2 \sim 1/N^8$, therefore it is justified to take γ a constant in our calculation. When γ is nonzero but small, the RG flows will only change quantitatively. For instance, expanded to the first order of γ , the scaling dimensions of the three eigenvectors of the RG equation at the stable fixed point become $\Delta_1 = -\epsilon$, $\Delta_2 = -\epsilon + \frac{4448\epsilon}{567N} + \frac{2849936\epsilon\gamma}{3988845}$, $\Delta_3 = -\epsilon + \frac{24950\epsilon}{567N} - \frac{30088528\epsilon\gamma}{27921915N}$, and the scaling dimension of r becomes $[r] = \frac{1}{\nu} = 2 - \epsilon + \frac{158\epsilon}{7N} - \frac{1032\epsilon\gamma}{1715N}$.

If we take $N = 1$, the v and w terms are identical. In this case in addition to the trivial Gaussian fixed

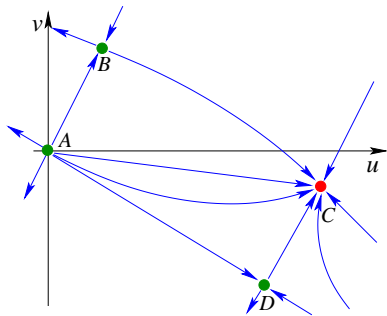


FIG. 2: The schematic RG flow diagram for equation Eq. 9 in the large- N limit with $w = w_* = \frac{3\epsilon}{7N}$. The four fixed points are $A, (u_*, v_*) = (0, 0)$; $B, (\frac{\epsilon}{24N}, \frac{\epsilon}{12N})$; $C, (\frac{17\epsilon}{84N}, -\frac{\epsilon}{42N})$; and $D, (\frac{9\epsilon}{56N}, -\frac{3\epsilon}{28N})$. C is the stable fixed point.

point, there is only one other fixed point at $v_* = 2u_* = \epsilon/34$ with $O(3)$ flavor-space combined rotation symmetry, which is the same fixed point as the ferromagnetic transition with dipolar interaction [10, 11]. In 3d space, the dipolar interaction also projects a spin wave to its transverse direction. The dipolar fixed point is unstable against the $O(3)$ to cubic symmetry breaking, therefore when $N = 1$ our first order ϵ expansion predicts a first order transition. We already mentioned that the case with $N = 1$ is equivalent to the CDM-3. However, in our GL formalism, in the ordered phase, the power law spin-spin correlation still persists if the long range correlation is subtracted. For instance, the fluctuation $\delta\phi_\mu = \phi_\mu - \langle\phi_\mu\rangle$ is still subject to the constraint $\sum_\mu \nabla_\mu \delta\phi_\mu = 0$, therefore although the fluctuation is gapped, it still leads to the $1/r^3$ power-law correlation. But in CDM, the ordered phase only has short range connected dimer correlation on top of the long range order [12]. This difference is due to the fact that our formalism does not encode the discreteness of the dimers. Therefore one possible scenario for the CDM-3 with staggered ground state is that, if we lower the temperature from the Coulomb phase, after the first order transition of ϕ^a , there has to be another ‘‘Higgs’’ like phase transition that destroys the power-law connected correlation. Or there can be one single strong first order transition that connects the Coulomb phase and staggered dimer crystal directly.

The $J_1 - J_2$ model Eq. 3 is invariant under cubic symmetry transformation. One can turn on various types of cubic symmetry breaking anisotropy to this model, and the energy favors one of the three flavors of vector field ϕ_μ^a to order. Let us assume ϕ_z^a is ordered at low temperature. To describe this transition we can turn on an extra mass gap m for ϕ_x^a and ϕ_y^a in Eq. 6, and by taking the limit $g \rightarrow \infty$, at the critical point $r = 0$ the renormalized correlation function for ϕ_z^a becomes

$$\langle\phi_z^a(\vec{q})\phi_z^b(-\vec{q})\rangle \sim \frac{\delta_{ab}}{m\frac{q_z^2}{q_x^2+q_y^2} + q_x^2 + q_y^2 + \dots}. \quad (13)$$

In this correlation function the scaling dimension $[q_z] = 2[q_x] = 2[q_y] = 2$, therefore this transition is effectively a $z = 2$ transition, and \mathcal{F}_4 is marginal according to power-counting. This cubic symmetry breaking situation has been studied in Ref. [13].

In this work we studied the transition between high temperature Coulomb phase and the low temperature staggered spin ordered phase in the $O(N)$ spin-ice model. Higher order ϵ and $1/N$ expansion are demanded to obtain more quantitatively accurate results. The model Eq. 3 can be simulated directly numerically, and our RG calculation can be tested. The columnar phase with $J_1 > 0$ and $J_2 < 0$ is also interesting. But since the columnar order does not correspond to the uniform order of ϕ_μ^a , the order parameter description is more complicated. We will study this situation in future.

The CDM is also considered as a simple analogue of the spin-ice materials such as $\text{Ho}_2\text{Ti}_2\text{O}_7$ and $\text{Dy}_2\text{Ti}_2\text{O}_7$ [14, 15, 16], where the Ho^{3+} and Dy^{3+} magnetic moments reside on the sites of a pyrochlore lattice, and the ground state of these moments satisfies the same ice-rule constraint as Eq. 2. The Coulomb phase of the spin ice materials with fractionalized ‘‘monopole’’ like defect excitation has been observed experimentally [17]. The formalism developed in our work is largely applicable to the pyrochlore lattice, while the symmetry analysis and the number of quartic terms are different. A complete symmetry analysis is demanded in order to correctly understand the $O(N)$ spin-ice on the pyrochlore lattice.

The author thanks very helpful discussion with Leon Balents, Subir Sachdev and T. Senthil. This work is sponsored by the Society of Fellows, Harvard University.

-
- [1] D. A. Huse, W. Krauth, R. Moessner, and S. L. Sondhi, Phys. Rev. Lett. **91**, 167004 (2003).
 - [2] G. Chen, J. Gukelberger, S. Trebst, F. Alet, and L. Balents, Phys. Rev. B **80**, 045112 (2009).
 - [3] F. Alet, G. Misguich, V. Pasquier, R. Moessner, and J. L. Jacobsen, Phys. Rev. Lett. **97**, 030403 (2006).
 - [4] G. Misguich, V. Pasquier, and F. Alet, Phys. Rev. B **78**, 100402(R) (2008).
 - [5] R. Moessner and S. L. Sondhi, Phys. Rev. B **68**, 184512 (2003).
 - [6] M. Hermele, T. Senthil, and M.P.A. Fisher, Phys. Rev. B. **72**, 104404 (2005).
 - [7] S. Powell and J. T. Chalker, Phys. Rev. Lett. **101**, 155702 (2008).
 - [8] L. Pauling, Journal of the American Chemical Society **57**, 2680 (1935).
 - [9] C. L. Henley, Phys. Rev. Lett. **62**, 2056 (1989).
 - [10] M. E. Fisher and A. Aharony, Phys. Rev. Lett. **30**, 559 (1973).
 - [11] A. Aharony and M. E. Fisher, Phys. Rev. B **8**, 3323 (1973).
 - [12] The author is grateful to Leon Balents for pointing this out.

- [13] T. S. Pickles, T. E. Saunders, and J. T. Chalker, Europhysics Letters **84**, 36002 (2008).
- [14] P. W. Anderson, Phys. Rev. **102**, 1008 (1956).
- [15] S. V. Isakov, R. Moessner, and S. L. Sondhi, Phys. Rev. Lett. **95**, 217201 (2005).
- [16] C. Castelnovo, R. Moessner, and S. L. Sondhi, Nature **451**, 42 (2008).
- [17] T. Fennell, P. P. Deen, A. R. Wildes, K. Schmalzl, D. Prabhakaran, A. T. Boothroyd, R. J. Aldus, D. F. McMorrow, and S. T. Bramwell, Science **326**, 415 (2009).